

Projective Dynamics Analysis of Magnetization Reversal

Gregory Brown^{a,*}, M. A. Novotny^b, Per Arne Rikvold^c

^a *Center for Computational Sciences, Oak Ridge National Lab,
Oak Ridge, TN 37831-6114, USA*

*School of Computational Science and Information Technology,
Florida State University, Tallahassee, FL 32306-4120, USA*

^b *Department of Physics and Astronomy and
ERC Center for Computational Sciences,
Mississippi State University, MS 39762, USA*

^c *Department of Physics, CSIT, and MARTECH,
Florida State University, Tallahassee, FL 32303-4350, USA*

Abstract

The computational Projective Dynamics method is used to analyze simulations of magnetization reversal in nanoscale magnetic pillars. It is shown that this method can be used to determine the magnetizations corresponding to the metastable minimum and saddle point in the free energy, and the free-energy barrier associated with those points. For the nanopillars studied here, entropy is found to provide a significant contribution to the free-energy barrier which determines the reversal time scale.

Key words: Magnetization Reversal, Projective Dynamics, Micromagnetics

Understanding magnetization reversal is important for technological applications where the magnetic orientation of nanoscale regions must be quickly assigned. For information storage, two configurations of the magnetization are used to encode the state of a bit of data. During the assignment process, strong fields are applied to create a free-energy minimum for only one of these configurations, and the bit almost certainly assumes the equilibrium configuration. For weaker fields, the two configurations correspond to local free-energy minima separated by a free-energy maximum. The minimum corresponding to a

* Corresponding author. FAX: +1-850-644-0098

Email address: Email: brownrg@csit.fsu.edu. (Gregory Brown).

magnetization parallel to the applied field is truly stable, while the antiparallel minimum is higher in energy and therefore metastable. In this situation the configuration depends not only on the relative weights of the minima, but for device and human time scales, it also depends on the history of the configuration. At some point along the most probable path between the minima there must occur a free-energy maximum in the form of a saddle point. The free-energy difference between the maximum and either minimum, often called a free-energy barrier, determines the time scale for transitions of the configuration from that minimum to the other.

To a first approximation these barriers and the curvature of the free energy near the extrema control the nonequilibrium dynamics of a system. Thus locating free-energy extrema is essential for developing a detailed understanding of the dynamics of metastable states, and that understanding is important for such things as maximizing data integrity and enabling the technology of hybrid recording [1], which uses lower-than-coercive applied fields to assign magnetic orientations in high-coercivity magnetic materials. While the free-energy minima can be easily located, the saddle point has proven much harder to measure [2]. Here we present results using the Projective Dynamics method [3,4,5] to probe the magnetization reversal of high-aspect-ratio nanoscale model magnets.

It has already been shown that the Projective Dynamics method can be used to locate the saddle point [4,6,7]. The method involves projecting the original description of the dynamics in terms of a large number of variables onto a stochastic description in terms of one variable. For example, the dynamics of the thousands of individual spins in a nanoscale pillar can be projected onto the stochastic dynamics of the total magnetization along the long axis of the nanomagnet, M_z . The transition rates between values of M_z are measured by the probabilities P_{grow} , which correspond to an increase in the volume of stable magnetization, and P_{shrink} , which correspond to a decrease in the volume. For values of M_z with $P_{\text{grow}} > P_{\text{shrink}}$, on average the volume of the stable magnetization grows. This corresponds to a negative local slope for the free energy. Likewise, $P_{\text{grow}} < P_{\text{shrink}}$ corresponds to a positive local slope. Values of M_z for which $P_{\text{grow}} = P_{\text{shrink}}$ correspond to zero slope, *i.e.* extrema of the free energy. Crossings of P_{grow} and P_{shrink} , then, can be used to determine the locations of the extrema, including the saddle point.

Here we present results for Projective Dynamics applied to micromagnetic simulations of magnetization reversal in a chain of 17 spins, \vec{S}_i , with the chain aligned along the z -axis [8]. Using an extended Heisenberg model, the internal energy of the system is given by

$$E = -J \sum_{i=1}^{16} \hat{S}_i \cdot \hat{S}_{i+1} - \frac{D}{2} \sum_i \sum_{j \neq i} \frac{[3\hat{z}(\hat{z} \cdot \hat{S}_j) - \hat{S}_j] \cdot \hat{S}_i}{|j-i|^3} + B \sum_i S_{i,z}, \quad (1)$$

where J is the exchange energy, B is the strength of the external field oriented parallel to $-\hat{z}$, and D is the strength of the dipole-dipole interactions in energy units, see Eqs. (17) and (18) of Ref. [9]. We choose parameters consistent with previous studies of iron nanopillars modeled as a one-dimensional chain of spins [7,8,9,10]: $J=1.6 \times 10^{-12}$ erg and $D=4.1 \times 10^{-12}$ erg. The dynamics consist of each spin precessing around a local field, i.e. the Landau-Lifshitz-Gilbert (LLG) equation [11,12]

$$\frac{d\hat{S}_i}{dt} = \frac{\gamma_0}{1 + \alpha^2} \hat{S}_i \times [\vec{H}_i - \alpha \hat{S}_i \times \vec{H}_i] , \quad (2)$$

where the scaled electron gyromagnetic ratio $\gamma_0 = 9.26 \times 10^{21}$ Hz/erg for this system, and the local field is given by the functional derivative $\vec{H}_i = -\delta E / \delta \vec{S}_i$. The phenomenological damping parameter $\alpha = 0.1$ was chosen to give underdamped dynamics, and an Euler integration scheme was used [13].

Dipole-dipole interactions make head-to-tail alignment of the spins along the chain favorable and provide a strong uniaxial anisotropy for this system. For each simulated reversal, the nanopillar was allowed to come to equilibrium in a field $B_0=1.9 \times 10^{-12}$ erg (1000 Oe). Then the magnitude of B was quickly decreased to a value of $-B_0$ to create a metastable configuration of the magnetization. For each integration step, data for P_{grow} , P_{shrink} , and the energy were binned on M_z . Results for this system have been presented previously [7]. Here we present improved results obtained from a systematic choice in bin width and from including lower temperatures.

Projective dynamics is most easily analyzed for discrete systems, such as the Ising model with spin-flip dynamics. Then M_z changes by $-S$, 0, or $+S$ at each step, and the stochastic dynamics are easy to analyze in terms of jumps along a well-defined chain of states. When M_z is a continuous variable, binning is used to create the chain of states. However, there are competing limitations that determine the bin size. One is the assumption of complete mixing within a bin, which is required for the transitions between bins to be a Markov process. If the bins are too large, then complete mixing within the bins will not be present and there will be memory effects. Another limiting effect is gathering enough statistics in each bin to measure the probabilities P_{grow} and P_{shrink} . If the bins are too small, there will be inadequate statistics related to these measured probabilities. Furthermore, we would like to have the projected Markov matrix be tridiagonal, which allows calculation of residence times using Eq.(3), introduced below, rather than inverting a large matrix. Tridiagonality of the Markov matrix requires that jumps from anywhere in the bin can go only into the bin with the next largest or smallest z -component of the magnetization.

The results presented in this work were obtained in the following manner. Data were collected for on the order of 10^2 switches for each temperature with a bin

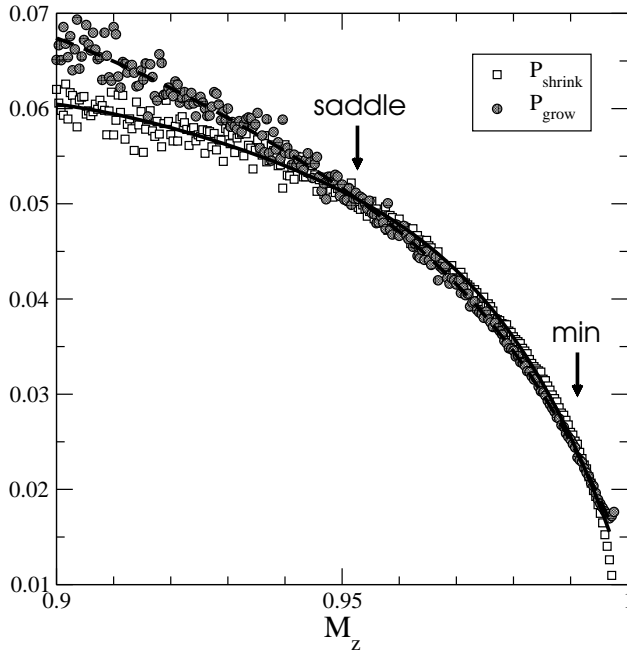


Fig. 1. Probability of shrinking, P_{shrink} , (squares) and growing, P_{grow} , (circles) for $T=5$ K. The solid curves are fifth-order polynomial fits to the data. The locations of the metastable minimum and saddle point, as indicated by the arrows, are determined from the intersections of the polynomials.

of width $b=5 \times 10^{-5}$. The data were then analyzed for bin widths of b , $2b$, $3b$, etc. until jumps only occurred between neighboring bins. Using this method, the optimal bin width was found to be $5b$ at $T=3$ K and $25b$ at $T=50$ K. In contrast, in Ref. [7] bins of width $100b$ were used. Both probabilities, P_{grow} (circles) and P_{shrink} (squares), for $T=5$ K, are shown in Fig. 1. Also shown are two fifth-order polynomials fit to these probabilities. Throughout this work, fifth-order polynomial fits have been used to determine the intersection of P_{grow} and P_{shrink} , and we find that the order of polynomial used affects the estimated location by less than 1% for the saddle point. The crossings for $T=5$ K are labeled with arrows in Fig. 1, with the crossing near $M_z=0.995$ the metastable minimum and that near $M_z=0.95$ the saddle point.

The values of M_z for the metastable minimum (circles) and the saddle point (diamonds) for all temperatures T are shown in Fig. 2. Similar results have been shown previously [6,7], but the results shown here are quantitatively different because of the smaller bins used. The changes are as large as 10% and are strongest for the saddle point. The linear dependence of the M_z of the saddle point on T noted previously [6,7] is present in the new data as well, but only for $T>5$ K. The solid line is a least-squares fit, and its intercept is $M_z=0.958$. The deviation from linearity at low temperature is expected to the

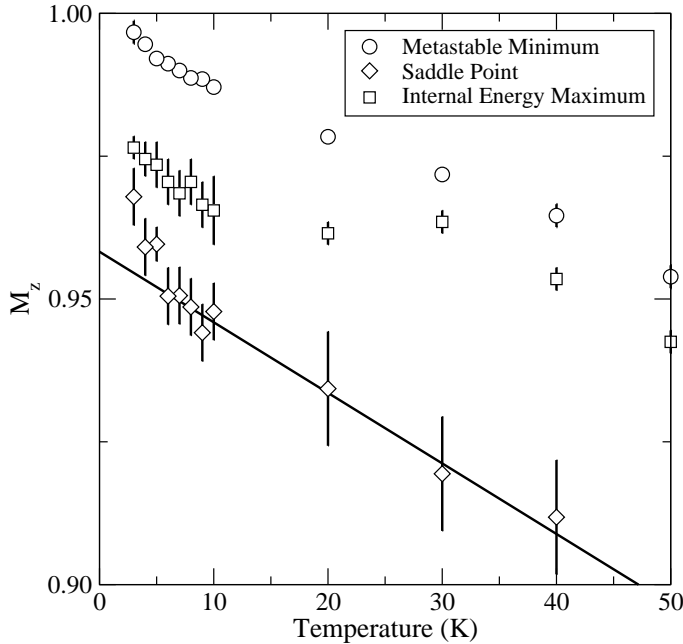


Fig. 2. M_z of metastable minimum (circles), internal energy maximum (squares), and saddle point (diamonds) vs temperature. The separation between the saddle point and the internal-energy maximum implies large entropic effects in magnetization reversal. The solid line is a least-squares fit to the saddle-point data. The metastable minimum is identically unity at $T=0$ K.

extent that extrapolation of the linear fit to $T=0$ K is not consistent with the internal-energy maximum, described below. This deviation was not seen in previous studies since such low temperatures are considered here for the first time.

The free energy, $F=E - TS$, has contributions from the internal energy and the entropy, S . When the temperature is exactly zero, there is no entropic contribution to the free energy, and the saddle point corresponds to the maximum in the internal energy. The results for the maximum of the average internal energy, $\langle E \rangle$, binned on M_z are shown (squares) in Fig. 2. The M_z for the saddle point and the internal-energy maximum converge as the temperature decreases, as expected. The separation between M_z at the internal-energy maximum and the saddle point at fixed T is a measure of the importance of entropic contributions to the magnetization reversal process. The separation in Fig. 2 indicates that entropy is quite important in these model nanopillars.

The internal-energy “barrier”, the difference between $\langle E \rangle$ at the saddle point and the metastable minimum, is shown vs temperature T in Fig. 3 as squares. Note that for all but the lowest temperatures the difference is negative, indi-

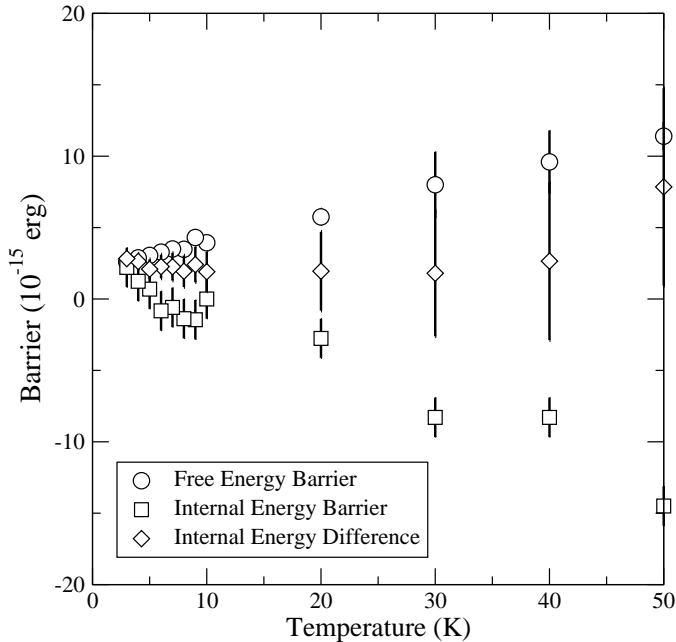


Fig. 3. The free-energy barrier (circles) and internal-energy barrier (squares) vs temperature. The difference between the two barriers is due to entropic contributions and vanished as $T \rightarrow 0$. The difference between the maximum internal energy and the internal energy at the metastable minimum (diamonds) is also shown.

cating that the $\langle E \rangle$ for the saddle point is *lower* than that of the metastable minimum. It is indeed possible for a system to be metastable in this situation, because it is a *free-energy* barrier that is actually required. The free-energy barrier can be estimated using Projective Dynamics from the time spent in each bin i , $h(i)$, which is proportional to the Boltzmann factor $\exp(-F(i)/k_B T)$. For a tridiagonal Markov matrix, the residence time $h(i)$ can be found from the growing and shrinking probabilities by [4,5,3]

$$h(i) = [1 + P_{\text{shrink}}(i-1)h(i-1)] / P_{\text{grow}}(i) , \quad (3)$$

with $h(1) = 1/P_{\text{grow}}(1)$, where we take the first bin to be the stable state and iterate Eq. (3) towards the metastable state. (Note that the cited references iterate from the metastable to stable state.) free-energy barrier is $\Delta F = k_B T \ln(h(i_{\text{min}})/h(i_{\text{saddle}}))$, where i_{min} is the bin containing the metastable minimum and i_{saddle} contains the saddle point. The results for the free-energy barrier are shown (circles) in Fig. 3. The free-energy barrier is always positive and approaches the internal-energy barrier as $T \rightarrow 0$, as expected. However, it is clear from the internal-energy barrier being negative for most temperatures and from the temperature dependence of ΔF , that the entropy contributes significantly to the metastability. This indicates that the configuration of $\{S_i\}$

is relatively restricted at the saddle-point, and that this restriction is more important than the combined dipole-dipole and exchange energies at all but the smallest temperatures. The difference between the maximum $\langle E \rangle$ and the value at the metastable minimum is also shown in Fig. 3 as diamonds. This difference might easily be mistaken for the barrier to magnetization reversal, but here it is much less sensitive to the temperature than the measured free-energy barrier.

In this paper, the usefulness of Projective Dynamics for locating the metastable minimum and saddle point in magnetization reversal has been demonstrated. Once these points are known, it is also possible to directly find the free-energy barrier of the reversal process, also using Projective Dynamics, or the internal-energy barrier, using some other technique to find the internal energy. One of the truly exciting aspects of Projective Dynamics is that it is not limited to analyzing simulations. Since only data on the time-dependence of the slow variable is needed, the analysis can also be applied to experimental data.

This work was supported by the LDRD Program of ORNL, managed by UT-Battelle, LLC (U.S. DOE Contract No. DE-AC05-00OR22725), by the Computational Material Science Network of BES-DMSE, by the U.S. NSF (Grant 0120310), and by Florida State University.

References

- [1] J.J.M. Ruigrok, R. Coehoorn, S.R. Cumpson, H.W. Kesteren, *J. Appl. Phys.* 87 (2000) 5398.
- [2] W. E, W. Ren, E. Vanden-Eijnden, *J. Appl. Phys.* 93 (2003) 2275.
- [3] M. Kolesik, M.A. Novotny, P.A. Rikvold, *Phys. Rev. Lett.* 80 (1998) 3384.
- [4] M.A. Novotny, *Int. J. Mod. Phys. C* 10 (2000) 1483; M.A. Novotny, in: D. Stauffer (Ed.), *Annual Reviews of Computational Physics IX* (World Scientific, Singapore, 2001), p. 153.
- [5] S.J. Mitchell, M.A. Novotny, J.D. Muñoz, *Int. J. Mod. Phys. C* 10 (2000) 1503.
- [6] G. Brown, M. A. Novotny, P. A. Rikvold, in: D.P. Landau, S.P. Lewis, H.-B. Schüttler (Eds.), *Computer Simulation Studies in Condensed Matter Physics XV* (Springer, Berlin, 2003), p. 24.
- [7] G. Brown, M.A. Novotny, P.A. Rikvold, *J. Appl. Phys.* 93 (2003) 6817.
- [8] E.D. Boerner, H.N. Bertram, *IEEE Trans. Magn.* 33 (1997) 3052.
- [9] G. Brown, M.A. Novotny, P.A. Rikvold, *Phys. Rev. B* 64 (2001) 134422.

- [10] S. Wirth, M. Field, D.D. Awschalom, S. von Molnár, *Phys. Rev. B* 57 (1998) R14028; *J. Appl. Phys.* 85 (1999) 5249.
- [11] W.F. Brown, *Phys. Rev.* 130 (1963) 1677.
- [12] A. Aharoni, *Introduction to the Theory of Ferromagnetism* (Clarendon, Oxford, 1996).
- [13] X. Feng, P.B. Visscher, *J. Appl. Phys.* 91 (2002) 8712.